



# CHORUS

This is the accepted manuscript made available via CHORUS. The article has been published as:

## Measurement of higher cumulants of net-charge multiplicity distributions in Au+Au collisions at $\sqrt{s_{NN}}=7.7-200\text{GeV}$

A. Adare *et al.* (PHENIX Collaboration)

Phys. Rev. C **93**, 011901 — Published 19 January 2016

DOI: [10.1103/PhysRevC.93.011901](https://doi.org/10.1103/PhysRevC.93.011901)

1 Measurement of higher cumulants of net-charge multiplicity distributions in Au+Au  
2 collisions at  $\sqrt{s_{NN}} = 7.7\text{--}200$  GeV

3 A. Adare,<sup>13</sup> S. Afanasiev,<sup>31</sup> C. Aidala,<sup>40,44,45</sup> N.N. Ajitanand,<sup>65</sup> Y. Akiba,<sup>59,60</sup> R. Akimoto,<sup>12</sup> H. Al-Bataineh,<sup>53</sup>  
4 J. Alexander,<sup>65</sup> H. Al-Ta'ani,<sup>53</sup> A. Angerami,<sup>14</sup> K. Aoki,<sup>33,36,59</sup> N. Apadula,<sup>29,66</sup> Y. Aramaki,<sup>12,59</sup> H. Asano,<sup>36,59</sup>  
5 E.C. Aschenauer,<sup>7</sup> E.T. Atomssa,<sup>37,66</sup> R. Averbeck,<sup>66</sup> T.C. Awes,<sup>55</sup> B. Azmoun,<sup>7</sup> V. Babintsev,<sup>25</sup> M. Bai,<sup>6</sup>  
6 G. Baksay,<sup>20</sup> L. Baksay,<sup>20</sup> B. Bannier,<sup>66</sup> K.N. Barish,<sup>8</sup> B. Bassalleck,<sup>52</sup> A.T. Basye,<sup>1</sup> S. Bathe,<sup>5,8,60</sup>  
7 V. Baublis,<sup>58</sup> C. Baumann,<sup>46</sup> S. Baumgart,<sup>59</sup> A. Bazilevsky,<sup>7</sup> S. Belikov,<sup>7,\*</sup> R. Belmont,<sup>13,45,70</sup> R. Bennett,<sup>66</sup>  
8 A. Berdnikov,<sup>62</sup> Y. Berdnikov,<sup>62</sup> A.A. Bickley,<sup>13</sup> D. Black,<sup>8</sup> D.S. Blau,<sup>35</sup> J.S. Bok,<sup>52,53,74</sup> K. Boyle,<sup>60,66</sup>  
9 M.L. Brooks,<sup>40</sup> J. Bryslawskij,<sup>5</sup> H. Buesching,<sup>7</sup> V. Bumazhnov,<sup>25</sup> G. Bunce,<sup>7,60</sup> S. Butsyk,<sup>40,52</sup> C.M. Camacho,<sup>40</sup>  
10 S. Campbell,<sup>14,66</sup> P. Castera,<sup>66</sup> C.-H. Chen,<sup>60,66</sup> C.Y. Chi,<sup>14</sup> M. Chiu,<sup>7</sup> I.J. Choi,<sup>26,74</sup> J.B. Choi,<sup>10</sup> S. Choi,<sup>64</sup>  
11 R.K. Choudhury,<sup>4</sup> P. Christiansen,<sup>42</sup> T. Chujo,<sup>69</sup> P. Chung,<sup>65</sup> O. Chvala,<sup>8</sup> V. Cianciolo,<sup>55</sup> Z. Citron,<sup>66,72</sup>  
12 B.A. Cole,<sup>14</sup> M. Connors,<sup>66</sup> P. Constantin,<sup>40</sup> N. Cronin,<sup>47,66</sup> N. Crossette,<sup>47</sup> M. Csanád,<sup>18</sup> T. Csörgő,<sup>73</sup>  
13 T. Dahms,<sup>66</sup> S. Dairaku,<sup>36,59</sup> I. Danchev,<sup>70</sup> K. Das,<sup>21</sup> A. Datta,<sup>44,52</sup> M.S. Daugherty,<sup>1</sup> G. David,<sup>7</sup>  
14 K. Dehmelt,<sup>20,66</sup> A. Denisov,<sup>25</sup> A. Deshpande,<sup>60,66</sup> E.J. Desmond,<sup>7</sup> K.V. Dharmawardane,<sup>53</sup> O. Dietzsch,<sup>63</sup>  
15 L. Ding,<sup>29</sup> A. Dion,<sup>29,66</sup> J.H. Do,<sup>74</sup> M. Donadelli,<sup>63</sup> L. D'Orazio,<sup>43</sup> O. Drapier,<sup>37</sup> A. Drees,<sup>66</sup> K.A. Drees,<sup>6</sup>  
16 J.M. Durham,<sup>40,66</sup> A. Durum,<sup>25</sup> D. Dutta,<sup>4</sup> S. Edwards,<sup>6,21</sup> Y.V. Efremenko,<sup>55</sup> F. Ellinghaus,<sup>13</sup> T. Engelmöre,<sup>14</sup>  
17 A. Enokizono,<sup>39,55,59,61</sup> H. En'yo,<sup>59,60</sup> S. Esumi,<sup>69</sup> K.O. Eyser,<sup>7,8</sup> B. Fadem,<sup>47</sup> D.E. Fields,<sup>52</sup> M. Finger,<sup>9</sup>  
18 M. Finger, Jr.,<sup>9</sup> F. Fleuret,<sup>37</sup> S.L. Fokin,<sup>35</sup> Z. Fraenkel,<sup>72,\*</sup> J.E. Frantz,<sup>54,66</sup> A. Franz,<sup>7</sup> A.D. Frawley,<sup>21</sup>  
19 K. Fujiwara,<sup>59</sup> Y. Fukao,<sup>59</sup> T. Fusayasu,<sup>49</sup> K. Gainey,<sup>1</sup> C. Gal,<sup>66</sup> P. Garg,<sup>3</sup> A. Garishvili,<sup>67</sup> I. Garishvili,<sup>39,67</sup>  
20 F. Giordano,<sup>26</sup> A. Glenn,<sup>13,39</sup> H. Gong,<sup>66</sup> X. Gong,<sup>65</sup> M. Gonin,<sup>37</sup> Y. Goto,<sup>59,60</sup> R. Granier de Cassagnac,<sup>37</sup>  
21 N. Grau,<sup>2,14</sup> S.V. Greene,<sup>70</sup> M. Grosse Perdekamp,<sup>26,60</sup> Y. Gu,<sup>65</sup> T. Gunji,<sup>12</sup> L. Guo,<sup>40</sup> H.-Å. Gustafsson,<sup>42,\*</sup>  
22 T. Hachiya,<sup>24,59</sup> J.S. Haggerty,<sup>7</sup> K.I. Hahn,<sup>19</sup> H. Hamagaki,<sup>12</sup> J. Hamblen,<sup>67</sup> R. Han,<sup>57</sup> J. Hanks,<sup>14,66</sup>  
23 E.P. Hartouni,<sup>39</sup> K. Hashimoto,<sup>59,61</sup> E. Haslum,<sup>42</sup> R. Hayano,<sup>12</sup> S. Hayashi,<sup>12</sup> X. He,<sup>22</sup> M. Heffner,<sup>39</sup>  
24 T.K. Hemmick,<sup>66</sup> T. Hester,<sup>8</sup> J.C. Hill,<sup>29</sup> M. Hohlmann,<sup>20</sup> R.S. Hollis,<sup>8</sup> W. Holzmann,<sup>14</sup> K. Homma,<sup>24</sup> B. Hong,<sup>34</sup>  
25 T. Horaguchi,<sup>24,69</sup> Y. Hori,<sup>12</sup> D. Hornback,<sup>67</sup> S. Huang,<sup>70</sup> T. Ichihara,<sup>59,60</sup> R. Ichimiya,<sup>59</sup> J. Ide,<sup>47</sup> H. Iinuma,<sup>33</sup>  
26 Y. Ikeda,<sup>59,69</sup> K. Imai,<sup>30,36,59</sup> Y. Imazu,<sup>59</sup> J. Imrek,<sup>17</sup> M. Inaba,<sup>69</sup> A. Iordanova,<sup>8</sup> D. Isenhower,<sup>1</sup> M. Ishihara,<sup>59</sup>  
27 A. Isinhue,<sup>47</sup> T. Isobe,<sup>12,59</sup> M. Issah,<sup>70</sup> A. Isupov,<sup>31</sup> D. Ivanishchev,<sup>58</sup> B.V. Jacak,<sup>66</sup> M. Javani,<sup>22</sup> J. Jia,<sup>7,65</sup>  
28 X. Jiang,<sup>40</sup> J. Jin,<sup>14</sup> B.M. Johnson,<sup>7</sup> K.S. Joo,<sup>48</sup> D. Jouan,<sup>56</sup> D.S. Jumper,<sup>1,26</sup> F. Kajihara,<sup>12</sup> S. Kametani,<sup>59</sup>  
29 N. Kamihara,<sup>60</sup> J. Kamin,<sup>66</sup> S. Kaneti,<sup>66</sup> B.H. Kang,<sup>23</sup> J.H. Kang,<sup>74</sup> J.S. Kang,<sup>23</sup> J. Kapustinsky,<sup>40</sup>  
30 K. Karatsu,<sup>36,59</sup> M. Kasai,<sup>59,61</sup> D. Kawall,<sup>44,60</sup> M. Kawashima,<sup>59,61</sup> A.V. Kazantsev,<sup>35</sup> T. Kempel,<sup>29</sup> J.A. Key,<sup>52</sup>  
31 P.K. Khandai,<sup>3</sup> A. Khanzadeev,<sup>58</sup> K.M. Kijima,<sup>24</sup> B.I. Kim,<sup>34</sup> C. Kim,<sup>34</sup> D.H. Kim,<sup>48</sup> D.J. Kim,<sup>32</sup> E. Kim,<sup>64</sup>  
32 E.-J. Kim,<sup>10</sup> H.J. Kim,<sup>74</sup> K.-B. Kim,<sup>10</sup> S.H. Kim,<sup>74</sup> Y.-J. Kim,<sup>26</sup> Y.K. Kim,<sup>23</sup> E. Kinney,<sup>13</sup> K. Kiriluk,<sup>13</sup>  
33 Á. Kiss,<sup>18</sup> E. Kistenev,<sup>7</sup> J. Klatsky,<sup>21</sup> D. Kleinjan,<sup>8</sup> P. Kline,<sup>66</sup> L. Kochenda,<sup>58</sup> Y. Komatsu,<sup>12,33</sup> B. Komkov,<sup>58</sup>  
34 M. Konno,<sup>69</sup> J. Koster,<sup>26,60</sup> D. Kotchetkov,<sup>52,54</sup> D. Kotov,<sup>58,62</sup> A. Kozlov,<sup>72</sup> A. Král,<sup>15</sup> A. Kravitz,<sup>14</sup> F. Krizek,<sup>32</sup>  
35 G.J. Kunde,<sup>40</sup> K. Kurita,<sup>59,61</sup> M. Kurosawa,<sup>59,60</sup> Y. Kwon,<sup>74</sup> G.S. Kyle,<sup>53</sup> R. Lacey,<sup>65</sup> Y.S. Lai,<sup>14</sup> J.G. Lajoie,<sup>29</sup>  
36 A. Lebedev,<sup>29</sup> B. Lee,<sup>23</sup> D.M. Lee,<sup>40</sup> J. Lee,<sup>19</sup> K. Lee,<sup>64</sup> K.B. Lee,<sup>34,40</sup> K.S. Lee,<sup>34</sup> S.H. Lee,<sup>66</sup> S.R. Lee,<sup>10</sup>  
37 M.J. Leitch,<sup>40</sup> M.A.L. Leite,<sup>63</sup> M. Leitgab,<sup>26</sup> E. Leitner,<sup>70</sup> B. Lenzi,<sup>63</sup> B. Lewis,<sup>66</sup> X. Li,<sup>11</sup> P. Liebing,<sup>60</sup> S.H. Lim,<sup>74</sup>  
38 L.A. Linden Levy,<sup>13,39</sup> T. Liška,<sup>15</sup> A. Litvinenko,<sup>31</sup> H. Liu,<sup>40,53</sup> M.X. Liu,<sup>40</sup> B. Love,<sup>70</sup> R. Luechtenborg,<sup>46</sup>  
39 D. Lynch,<sup>7</sup> C.F. Maguire,<sup>70</sup> Y.I. Makdisi,<sup>6</sup> M. Makek,<sup>72,75</sup> A. Malakhov,<sup>31</sup> M.D. Malik,<sup>52</sup> A. Manion,<sup>66</sup>  
40 V.I. Manko,<sup>35</sup> E. Mannel,<sup>7,14</sup> Y. Mao,<sup>57,59</sup> T. Maruyama,<sup>30</sup> H. Masui,<sup>69</sup> S. Masumoto,<sup>12,33</sup> F. Matathias,<sup>14</sup>  
41 M. McCumber,<sup>13,40,66</sup> P.L. McGaughey,<sup>40</sup> D. McGlinchey,<sup>13,21</sup> C. McKinney,<sup>26</sup> N. Means,<sup>66</sup> A. Meles,<sup>53</sup>  
42 M. Mendoza,<sup>8</sup> B. Meredith,<sup>26</sup> Y. Miake,<sup>69</sup> T. Mibe,<sup>33</sup> J. Midori,<sup>24</sup> A.C. Mignerey,<sup>43</sup> P. Mikeš,<sup>9,28</sup> K. Miki,<sup>59,69</sup>  
43 A. Milov,<sup>7,72</sup> D.K. Mishra,<sup>4</sup> M. Mishra,<sup>3</sup> J.T. Mitchell,<sup>7</sup> Y. Miyachi,<sup>59,68</sup> S. Miyasaka,<sup>59,68</sup> A.K. Mohanty,<sup>4</sup>  
44 S. Mohapatra,<sup>65</sup> H.J. Moon,<sup>48</sup> Y. Morino,<sup>12</sup> A. Morreale,<sup>8</sup> D.P. Morrison,<sup>7,†</sup> M. Moskowitz,<sup>47</sup> S. Motschwiller,<sup>47</sup>  
45 T.V. Moukhanova,<sup>35</sup> T. Murakami,<sup>36,59</sup> J. Murata,<sup>59,61</sup> A. Mwai,<sup>65</sup> T. Nagae,<sup>36</sup> S. Nagamiya,<sup>33,59</sup> J.L. Nagle,<sup>13,‡</sup>  
46 M. Naglis,<sup>72</sup> M.I. Nagy,<sup>18,73</sup> I. Nakagawa,<sup>59,60</sup> Y. Nakamiya,<sup>24</sup> K.R. Nakamura,<sup>36,59</sup> T. Nakamura,<sup>33,59</sup>  
47 K. Nakano,<sup>59,68</sup> C. Nattrass,<sup>67</sup> A. Nederlof,<sup>47</sup> P.K. Netrakanti,<sup>4</sup> J. Newby,<sup>39</sup> M. Nguyen,<sup>66</sup> M. Nihashi,<sup>24,59</sup>  
48 T. Niida,<sup>69</sup> R. Nouicer,<sup>7,60</sup> N. Novitzky,<sup>32,66</sup> A. Nukariya,<sup>12</sup> A.S. Nyanin,<sup>35</sup> H. Obayashi,<sup>24</sup> E. O'Brien,<sup>7</sup>  
49 S.X. Oda,<sup>12</sup> C.A. Ogilvie,<sup>29</sup> M. Oka,<sup>69</sup> K. Okada,<sup>60</sup> Y. Onuki,<sup>59</sup> A. Oskarsson,<sup>42</sup> M. Ouchida,<sup>24,59</sup> K. Ozawa,<sup>12,33</sup>  
50 R. Pak,<sup>7</sup> V. Pantuev,<sup>27,66</sup> V. Papavassiliou,<sup>53</sup> B.H. Park,<sup>23</sup> I.H. Park,<sup>19</sup> J. Park,<sup>10,64</sup> S. Park,<sup>64</sup> S.K. Park,<sup>34</sup>  
51 W.J. Park,<sup>34</sup> S.F. Pate,<sup>53</sup> L. Patel,<sup>29</sup> H. Pei,<sup>29</sup> J.-C. Peng,<sup>26</sup> H. Pereira,<sup>16</sup> D.V. Perepelitsa,<sup>7,14</sup> V. Peresedov,<sup>31</sup>  
52 D.Yu. Peressounko,<sup>35</sup> R. Petti,<sup>7,66</sup> C. Pinkenburg,<sup>7</sup> R.P. Pisani,<sup>7</sup> M. Proissl,<sup>66</sup> M.L. Purschke,<sup>7</sup> A.K. Purwar,<sup>40</sup>

53 H. Qu,<sup>1,22</sup> J. Rak,<sup>32</sup> A. Rakotozafindrabe,<sup>37</sup> I. Ravinovich,<sup>72</sup> K.F. Read,<sup>55,67</sup> K. Reygers,<sup>46</sup> D. Reynolds,<sup>65</sup>  
 54 V. Riabov,<sup>51,58</sup> Y. Riabov,<sup>58,62</sup> E. Richardson,<sup>43</sup> N. Riveli,<sup>54</sup> D. Roach,<sup>70</sup> G. Roche,<sup>41,\*</sup> S.D. Rolnick,<sup>8</sup>  
 55 M. Rosati,<sup>29</sup> C.A. Rosen,<sup>13</sup> S.S.E. Rosendahl,<sup>42</sup> P. Rosnet,<sup>41</sup> P. Rukoyatkin,<sup>31</sup> P. Ružička,<sup>28</sup> M.S. Ryu,<sup>23</sup>  
 56 B. Sahlmueller,<sup>46,66</sup> N. Saito,<sup>33</sup> T. Sakaguchi,<sup>7</sup> K. Sakashita,<sup>59,68</sup> H. Sako,<sup>30</sup> V. Samsonov,<sup>51,58</sup> M. Sano,<sup>69</sup>  
 57 S. Sano,<sup>12,71</sup> M. Sarsour,<sup>22</sup> S. Sato,<sup>30,33</sup> T. Sato,<sup>69</sup> S. Sawada,<sup>33</sup> K. Sedgwick,<sup>8</sup> J. Seele,<sup>13</sup> R. Seidl,<sup>26,59,60</sup>  
 58 A.Yu. Semenov,<sup>29</sup> A. Sen,<sup>22,67</sup> R. Seto,<sup>8</sup> P. Sett,<sup>4</sup> D. Sharma,<sup>66,72</sup> I. Shein,<sup>25</sup> T.-A. Shibata,<sup>59,68</sup> K. Shigaki,<sup>24</sup>  
 59 M. Shimomura,<sup>29,50,69</sup> K. Shoji,<sup>36,59</sup> P. Shukla,<sup>4</sup> A. Sickles,<sup>7,26</sup> C.L. Silva,<sup>29,40,63</sup> D. Silvermyr,<sup>42,55</sup> C. Silvestre,<sup>16</sup>  
 60 K.S. Sim,<sup>34</sup> B.K. Singh,<sup>3</sup> C.P. Singh,<sup>3</sup> V. Singh,<sup>3</sup> M. Skolnik,<sup>47</sup> M. Slunečka,<sup>9</sup> S. Solano,<sup>47</sup> R.A. Soltz,<sup>39</sup>  
 61 W.E. Sondheim,<sup>40</sup> S.P. Sorensen,<sup>67</sup> I.V. Sourikova,<sup>7</sup> N.A. Sparks,<sup>1</sup> P.W. Stankus,<sup>55</sup> P. Steinberg,<sup>7</sup> E. Stenlund,<sup>42</sup>  
 62 M. Stepanov,<sup>44,53,\*</sup> A. Ster,<sup>73</sup> S.P. Stoll,<sup>7</sup> T. Sugitate,<sup>24</sup> A. Sukhanov,<sup>7</sup> J. Sun,<sup>66</sup> J. Sziklai,<sup>73</sup> E.M. Takagui,<sup>63</sup>  
 63 A. Takahara,<sup>12</sup> A. Taketani,<sup>59,60</sup> R. Tanabe,<sup>69</sup> Y. Tanaka,<sup>49</sup> S. Taneja,<sup>66</sup> K. Tanida,<sup>36,59,60,64</sup> M.J. Tannenbaum,<sup>7</sup>  
 64 S. Tarafdar,<sup>3,72</sup> A. Taranenko,<sup>51,65</sup> P. Tarján,<sup>17</sup> E. Tennant,<sup>53</sup> H. Themann,<sup>66</sup> T.L. Thomas,<sup>52</sup> T. Todoroki,<sup>59,69</sup>  
 65 M. Togawa,<sup>36,59</sup> A. Toia,<sup>66</sup> L. Tomášek,<sup>28</sup> M. Tomášek,<sup>15,28</sup> H. Torii,<sup>24</sup> R.S. Towell,<sup>1</sup> I. Tserruya,<sup>72</sup>  
 66 Y. Tsuchimoto,<sup>12,24</sup> T. Tsuji,<sup>12</sup> C. Vale,<sup>7,29</sup> H. Valle,<sup>70</sup> H.W. van Hecke,<sup>40</sup> M. Vargyas,<sup>18</sup> E. Vazquez-Zambrano,<sup>14</sup>  
 67 A. Veicht,<sup>14,26</sup> J. Velkovska,<sup>70</sup> R. Vértesi,<sup>17,73</sup> A.A. Vinogradov,<sup>35</sup> M. Virius,<sup>15</sup> B. Voas,<sup>29</sup> A. Vossen,<sup>26</sup>  
 68 V. Vrba,<sup>15,28</sup> E. Vznuzdaev,<sup>58</sup> X.R. Wang,<sup>53,60</sup> D. Watanabe,<sup>24</sup> K. Watanabe,<sup>59,61,69</sup> Y. Watanabe,<sup>59,60</sup>  
 69 Y.S. Watanabe,<sup>12</sup> F. Wei,<sup>29,53</sup> R. Wei,<sup>65</sup> J. Wessels,<sup>46</sup> S. Whitaker,<sup>29</sup> S.N. White,<sup>7</sup> D. Winter,<sup>14</sup> S. Wolin,<sup>26</sup>  
 70 J.P. Wood,<sup>1</sup> C.L. Woody,<sup>7</sup> R.M. Wright,<sup>1</sup> M. Wysocki,<sup>13,55</sup> B. Xia,<sup>54</sup> W. Xie,<sup>60</sup> Y.L. Yamaguchi,<sup>12,59,66</sup>  
 71 K. Yamaura,<sup>24</sup> R. Yang,<sup>26</sup> A. Yanovich,<sup>25</sup> J. Ying,<sup>22</sup> S. Yokkaichi,<sup>59,60</sup> Z. You,<sup>40,57</sup> G.R. Young,<sup>55</sup>  
 72 I. Younus,<sup>38,52</sup> I.E. Yushmanov,<sup>35</sup> W.A. Zajc,<sup>14</sup> A. Zelenski,<sup>6</sup> C. Zhang,<sup>55</sup> S. Zhou,<sup>11</sup> and L. Zolin<sup>31</sup>

(PHENIX Collaboration)

<sup>1</sup>Abilene Christian University, Abilene, Texas 79699, USA

<sup>2</sup>Department of Physics, Augustana University, Sioux Falls, South Dakota 57197, USA

<sup>3</sup>Department of Physics, Banaras Hindu University, Varanasi 221005, India

<sup>4</sup>Bhabha Atomic Research Centre, Bombay 400 085, India

<sup>5</sup>Baruch College, City University of New York, New York, New York, 10010 USA

<sup>6</sup>Collider-Accelerator Department, Brookhaven National Laboratory, Upton, New York 11973-5000, USA

<sup>7</sup>Physics Department, Brookhaven National Laboratory, Upton, New York 11973-5000, USA

<sup>8</sup>University of California-Riverside, Riverside, California 92521, USA

<sup>9</sup>Charles University, Ovocný trh 5, Praha 1, 116 36, Prague, Czech Republic

<sup>10</sup>Chonbuk National University, Jeonju, 561-756, Korea

<sup>11</sup>Science and Technology on Nuclear Data Laboratory, China Institute of Atomic Energy, Beijing 102413, People's Republic of China

<sup>12</sup>Center for Nuclear Study, Graduate School of Science, University of Tokyo, 7-3-1 Hongo, Bunkyo, Tokyo 113-0033, Japan

<sup>13</sup>University of Colorado, Boulder, Colorado 80309, USA

<sup>14</sup>Columbia University, New York, New York 10027 and Nevis Laboratories, Irvington, New York 10533, USA

<sup>15</sup>Czech Technical University, Zikova 4, 166 36 Prague 6, Czech Republic

<sup>16</sup>Dapnia, CEA Saclay, F-91191, Gif-sur-Yvette, France

<sup>17</sup>Debrecen University, H-4010 Debrecen, Egyetem tér 1, Hungary

<sup>18</sup>ELTE, Eötvös Loránd University, H-1117 Budapest, Pázmány P. s. 1/A, Hungary

<sup>19</sup>Ewha Womans University, Seoul 120-750, Korea

<sup>20</sup>Florida Institute of Technology, Melbourne, Florida 32901, USA

<sup>21</sup>Florida State University, Tallahassee, Florida 32306, USA

<sup>22</sup>Georgia State University, Atlanta, Georgia 30303, USA

<sup>23</sup>Hanyang University, Seoul 133-792, Korea

<sup>24</sup>Hiroshima University, Kagamiyama, Higashi-Hiroshima 739-8526, Japan

<sup>25</sup>IHEP Protvino, State Research Center of Russian Federation, Institute for High Energy Physics, Protvino, 142281, Russia

<sup>26</sup>University of Illinois at Urbana-Champaign, Urbana, Illinois 61801, USA

<sup>27</sup>Institute for Nuclear Research of the Russian Academy of Sciences, prospekt 60-letiya Oktyabrya 7a, Moscow 117312, Russia

<sup>28</sup>Institute of Physics, Academy of Sciences of the Czech Republic, Na Slovance 2, 182 21 Prague 8, Czech Republic

<sup>29</sup>Iowa State University, Ames, Iowa 50011, USA

<sup>30</sup>Advanced Science Research Center, Japan Atomic Energy Agency, 2-4 Shirakata Shirane, Tokai-mura, Naka-gun, Ibaraki-ken 319-1195, Japan

<sup>31</sup>Joint Institute for Nuclear Research, 141980 Dubna, Moscow Region, Russia

<sup>32</sup>Helsinki Institute of Physics and University of Jyväskylä, P.O.Box 35, FI-40014 Jyväskylä, Finland

<sup>33</sup>KEK, High Energy Accelerator Research Organization, Tsukuba, Ibaraki 305-0801, Japan

<sup>34</sup>Korea University, Seoul, 136-701, Korea

<sup>35</sup>National Research Center "Kurchatov Institute", Moscow, 123098 Russia

<sup>36</sup>Kyoto University, Kyoto 606-8502, Japan

<sup>37</sup> *Laboratoire Leprince-Ringuet, Ecole Polytechnique, CNRS-IN2P3, Route de Saclay, F-91128, Palaiseau, France*

<sup>38</sup> *Physics Department, Lahore University of Management Sciences, Lahore 54792, Pakistan*

<sup>39</sup> *Lawrence Livermore National Laboratory, Livermore, California 94550, USA*

<sup>40</sup> *Los Alamos National Laboratory, Los Alamos, New Mexico 87545, USA*

<sup>41</sup> *LPC, Université Blaise Pascal, CNRS-IN2P3, Clermont-Fd, 63177 Aubiere Cedex, France*

<sup>42</sup> *Department of Physics, Lund University, Box 118, SE-221 00 Lund, Sweden*

<sup>43</sup> *University of Maryland, College Park, Maryland 20742, USA*

<sup>44</sup> *Department of Physics, University of Massachusetts, Amherst, Massachusetts 01003-9337, USA*

<sup>45</sup> *Department of Physics, University of Michigan, Ann Arbor, Michigan 48109-1040, USA*

<sup>46</sup> *Institut für Kernphysik, University of Muenster, D-48149 Muenster, Germany*

<sup>47</sup> *Muhlenberg College, Allentown, Pennsylvania 18104-5586, USA*

<sup>48</sup> *Myongji University, Yongin, Kyonggido 449-728, Korea*

<sup>49</sup> *Nagasaki Institute of Applied Science, Nagasaki-shi, Nagasaki 851-0193, Japan*

<sup>50</sup> *Nara Women's University, Kita-uoya Nishi-machi Nara 630-8506, Japan*

<sup>51</sup> *National Research Nuclear University, MEPhI, Moscow Engineering Physics Institute, Moscow, 115409, Russia*

<sup>52</sup> *University of New Mexico, Albuquerque, New Mexico 87131, USA*

<sup>53</sup> *New Mexico State University, Las Cruces, New Mexico 88003, USA*

<sup>54</sup> *Department of Physics and Astronomy, Ohio University, Athens, Ohio 45701, USA*

<sup>55</sup> *Oak Ridge National Laboratory, Oak Ridge, Tennessee 37831, USA*

<sup>56</sup> *IPN-Orsay, Univ. Paris-Sud, CNRS/IN2P3, Université Paris-Saclay, BP1, F-91406, Orsay, France*

<sup>57</sup> *Peking University, Beijing 100871, People's Republic of China*

<sup>58</sup> *PNPI, Petersburg Nuclear Physics Institute, Gatchina, Leningrad region, 188300, Russia*

<sup>59</sup> *RIKEN Nishina Center for Accelerator-Based Science, Wako, Saitama 351-0198, Japan*

<sup>60</sup> *RIKEN BNL Research Center, Brookhaven National Laboratory, Upton, New York 11973-5000, USA*

<sup>61</sup> *Physics Department, Rikkyo University, 3-34-1 Nishi-Ikebukuro, Toshima, Tokyo 171-8501, Japan*

<sup>62</sup> *Saint Petersburg State Polytechnic University, St. Petersburg, 195251 Russia*

<sup>63</sup> *Universidade de São Paulo, Instituto de Física, Caixa Postal 66318, São Paulo CEP05315-970, Brazil*

<sup>64</sup> *Department of Physics and Astronomy, Seoul National University, Seoul 151-742, Korea*

<sup>65</sup> *Chemistry Department, Stony Brook University, SUNY, Stony Brook, New York 11794-3400, USA*

<sup>66</sup> *Department of Physics and Astronomy, Stony Brook University, SUNY, Stony Brook, New York 11794-3800, USA*

<sup>67</sup> *University of Tennessee, Knoxville, Tennessee 37996, USA*

<sup>68</sup> *Department of Physics, Tokyo Institute of Technology, Oh-okayama, Meguro, Tokyo 152-8551, Japan*

<sup>69</sup> *Center for Integrated Research in Fundamental Science and Engineering, University of Tsukuba, Tsukuba, Ibaraki 305, Japan*

<sup>70</sup> *Vanderbilt University, Nashville, Tennessee 37235, USA*

<sup>71</sup> *Waseda University, Advanced Research Institute for Science and Engineering, 17 Kikui-cho, Shinjuku-ku, Tokyo 162-0044, Japan*

<sup>72</sup> *Weizmann Institute, Rehovot 76100, Israel*

<sup>73</sup> *Institute for Particle and Nuclear Physics, Wigner Research Centre for Physics, Hungarian Academy of Sciences (Wigner RCP, RMKI) H-1525 Budapest 114, POBox 49, Budapest, Hungary*

<sup>74</sup> *Yonsei University, IPAP, Seoul 120-749, Korea*

<sup>75</sup> *University of Zagreb, Faculty of Science, Department of Physics, Bijenička 32, HR-10002 Zagreb, Croatia*

(Dated: December 21, 2015)

We report the measurement of cumulants ( $C_n, n = 1 \dots 4$ ) of the net-charge distributions measured within pseudorapidity ( $|\eta| < 0.35$ ) in Au+Au collisions at  $\sqrt{s_{NN}}=7.7\text{--}200$  GeV with the PHENIX experiment at the Relativistic Heavy Ion Collider. The ratios of cumulants (e.g.  $C_1/C_2, C_3/C_1$ ) of the net-charge distributions, which can be related to volume independent susceptibility ratios, are studied as a function of centrality and energy. These quantities are important to understand the quantum-chromodynamics phase diagram and possible existence of a critical end point. The measured values are very well described by expectation from negative binomial distributions. We do not observe any nonmonotonic behavior in the ratios of the cumulants as a function of collision energy. The measured values of  $C_1/C_2 = \mu/\sigma^2$  and  $C_3/C_1 = S\sigma^3/\mu$  can be directly compared to lattice quantum-chromodynamics calculations and thus allow extraction of both the chemical freeze-out temperature and the baryon chemical potential at each center-of-mass energy. The extracted baryon chemical potentials are in excellent agreement with a thermal-statistical analysis model.

PACS numbers: 25.75.Dw

\* Deceased

† PHENIX Co-Spokesperson: morrison@bnl.gov

‡ PHENIX Co-Spokesperson: jamie.nagle@colorado.edu

One of the main goals in the study of relativistic heavy ion collisions is to map the quantum chromodynamics (QCD) phase diagram at finite temperature ( $T$ ) and baryon chemical potential ( $\mu_B$ ) [1]. Although the exact nature of the phase transition at finite baryon density is still not well established, several models suggest that, at large  $\mu_B$  and low  $T$ , the phase transition between the hadronic phase and the quark-gluon-plasma (QGP) phase is of first order [2, 3] and that at high  $T$  and low  $\mu_B$  there is a simple cross over from the QGP to hadronic phase [4–8]. The point at which the first-order phase transition ends in the  $T - \mu_B$  plane is called the QCD critical end point (CEP), which is one of the central targets of the Relativistic Heavy Ion Collider (RHIC) beam-energy-scan program. Several calculations also reported the possible existence of the CEP in the  $T - \mu_B$  phase diagram [6, 7, 9].

RHIC at Brookhaven National Laboratory has provided a large amount of data from Au+Au collisions at different colliding energies, which gives us a unique opportunity to scan the  $T - \mu_B$  plane and investigate the possible existence and location of the CEP. In the thermodynamic limit, the correlation length ( $\xi$ ) diverges at the CEP [1]. Event-by-event fluctuations of various conserved quantities, such as net-baryon number, net-charge, and net-strangeness are proposed as possible signatures of the existence of the CEP [10–12]. It has been shown in lattice QCD that with a next-to-leading-order Taylor series expansion around vanishing chemical potentials, the cumulants of charge-fluctuations are sensitive indicators for the occurrence of a transition from the hadronic to QGP phase [13, 14]. Typically, the variances of net-baryon, net-charge, and net-strangeness distributions are proportional to  $\xi$  as  $\sigma^2(=C_2)=\langle(\delta N)^2\rangle\sim\xi^2$  [9], where  $N$  is the multiplicity,  $\delta N = N - \mu$  and  $\mu(=C_1)$  is the mean of the distribution.

Recent calculations reveal that higher cumulants of the fluctuations are much more sensitive to the proximity of the CEP than earlier measurements using second cumulants ( $\sigma^2$ ) [12, 15]. The skewness ( $S$ ) and kurtosis ( $\kappa$ ) are related to the third and fourth moments  $S(=C_3/C_2^{3/2})=\langle(\delta N)^3\rangle/\sigma^3\sim\xi^{4.5}$  and  $\kappa(=C_4/C_2^2)=\langle(\delta N)^4\rangle/\sigma^4-3\sim\xi^7$ . The ratio of the various order ( $n$ ) of cumulants ( $C_n$ ) and conventional values ( $\mu$ ,  $\sigma$ ,  $S$  and  $\kappa$ ) can be related as follows:  $\mu/\sigma^2=C_1/C_2$ ,  $S\sigma=C_3/C_2$ ,  $\kappa\sigma^2=C_4/C_2$ , and  $S\sigma^3/\mu=C_3/C_1$ . Because  $\xi$  diverges at the CEP, the ratios of cumulants  $S\sigma$  and  $\kappa\sigma^2$  should rise rapidly when approaching the CEP [16, 17]. The cumulants of conserved quantities of net-baryon, net-charge, and net-strangeness obtained from lattice QCD calculations [13, 14, 17] and a hadron resonance gas (HRG) model [18] are related to the generalized susceptibilities of  $n$ -th order ( $\chi^n$ ) associated with the conserved quantum numbers as  $\mu/\sigma^2\sim\chi^{(1)}/\chi^{(2)}$ ,  $S\sigma\sim\chi^{(3)}/\chi^{(2)}$ ,  $S\sigma^3/\mu\sim\chi^{(3)}/\chi^{(1)}$ , and  $\kappa\sigma^2\sim\chi^{(4)}/\chi^{(2)}$ . One advantage of measuring  $\mu/\sigma^2$ ,  $S\sigma$ ,  $S\sigma^3/\mu$ , and  $\kappa\sigma^2$  is that the volume dependence of  $\mu$ ,  $\sigma$ ,  $S$ , and  $\kappa$  cancel out in the ratios, hence theoretical calculations can be directly compared with the experimental measurements. These cumulant ratios can also be used to extract the freeze-out parameters and the location of the CEP [14]. Net-electric charge fluctuations are more straightforward to measure experimentally than net-baryon number fluctuations, which are partially accessible via net-proton measurement [19]. While net-charge fluctuations are not as sensitive as net-baryon fluctuations to the theoretical parameters, both measurements are desirable for a full understanding of the theory.

We report here precise measurements of the energy and centrality dependence of higher cumulants of net-charge multiplicity ( $\Delta N_{\text{ch}} = N^+ - N^-$ ) distributions measured by the PHENIX experiment at RHIC in Au+Au collisions at  $\sqrt{s_{NN}} = 7.7, 19.6, 27, 39, 62.4,$  and  $200$  GeV. These measurements cover a broad range of  $\mu_B$  in the QCD phase diagram.

The PHENIX detector is composed of two central spectrometer arms, two forward muon arms, and global detectors [20]. In this analysis, we use the central arm spectrometers, which cover a pseudorapidity range of  $|\eta| \leq 0.35$ . Each of the two arms subtends  $\pi/2$  radians in azimuth and is designed to detect charged hadrons, electrons, and photons. For data taken at  $\sqrt{s_{NN}} = 62.4$  and  $200$  GeV in 2010 and 2007, respectively, the event centrality is determined using total charge deposited in the beam-beam counters (BBC), which are also used for triggering and vertex determination. For lower energies ( $\sqrt{s_{NN}} = 39$  GeV and below) the acceptance of the BBCs ( $3.0 < |\eta| < 3.9$ ) are within the fragmentation region, so alternate detectors must be employed. For data taken at  $\sqrt{s_{NN}} = 39$  and  $7.7$  GeV in 2010, centrality is determined using the total charge deposited in the outer ring of the reaction plane detector (RXNP), which covers  $1.0 < |\eta| < 1.5$  [21]. For data taken at  $\sqrt{s_{NN}} = 19.6$  and  $27$  GeV in 2011, the RXNP was absent, so centrality is determined using the total energy of electromagnetic calorimeter (EMCal) clusters to minimize the correlation with the charge of the tracks measured in the same acceptance. More details on the procedure are given in [22]. The analyzed events for the above mentioned energies are within a collision vertex of  $|Z_{\text{vertex}}| < 30$  cm. The number of analyzed events are 2M, 6M, 21M, 154M, 474M, and 1681M for  $\sqrt{s_{NN}} = 7.7, 19.6, 27, 39, 62.4,$  and  $200$  GeV Au+Au collisions, respectively.

The number of positively charged ( $N^+$ ) and negatively charged ( $N^-$ ) particles measured on an event-by-event basis are used to calculate the net-charge ( $\Delta N_{\text{ch}}$ ) distributions for each collision centrality and energy. The charged-particle trajectories are reconstructed using information from the drift chamber and pad chambers (PC1 and PC3). A combination of reconstructed drift-chamber tracks and matching hits in PC1 are used to determine the momentum and charge of the particle. Tracks having a transverse momentum ( $p_T$ ) between  $0.3$  and  $2.0$  GeV/ $c$  are selected for this analysis. The ring imaging Čerenkov detector is used to reduce the electron background resulting from conversion photons. To further reduce the background, selected tracks are required to lie within a  $2.5\sigma$  matching window between track projections and PC3 hits, and a  $3\sigma$  matching window for the EMCal.

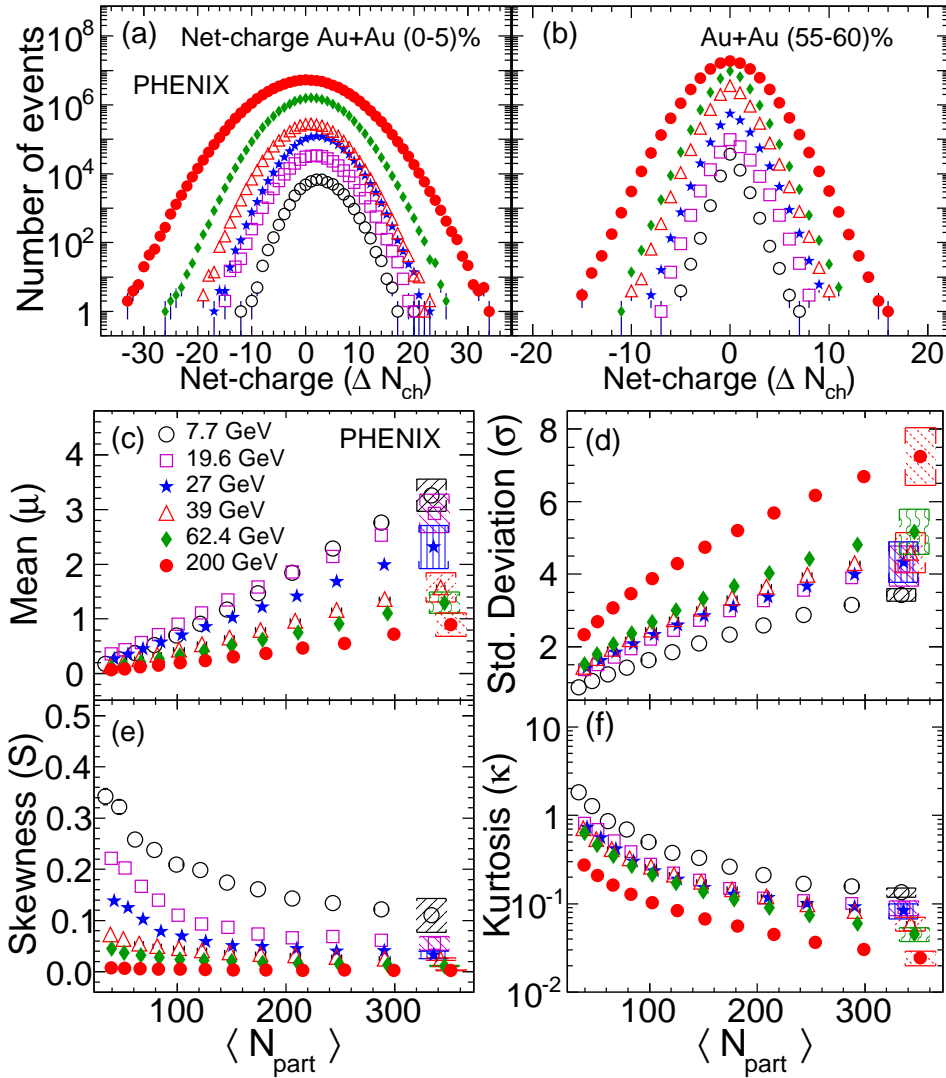


FIG. 1. (Color online). Uncorrected net-charge ( $\Delta N_{\text{ch}}$ ) distributions, within  $|\eta| \leq 0.35$  for different energies, from Au+Au collisions for (a) central (0%–5%) and (b) peripheral (55%–60%) centrality. (c)–(f) are the efficiency corrected cumulants of net-charge distributions as a function of  $\langle N_{\text{part}} \rangle$  from Au+Au collisions at different collision energies. Systematic uncertainties on moments are shown for central (0%–5%) collisions.

213 Figure 1(a) and (b) show  $\Delta N_{\text{ch}}$  distributions in Au+Au collisions for central (0%–5%) and peripheral (55%–60%)  
 214 collisions at different collision energies. These  $\Delta N_{\text{ch}}$  distributions are not corrected for reconstruction efficiency. The  
 215 centrality classes associated with the average number of participants ( $\langle N_{\text{part}} \rangle$ ) are defined for each 5% centrality bin.  
 216 These classes are determined using a Monte-Carlo simulation based on Glauber model calculations with the BBC,  
 217 RXNP, and EMCal detector response taken into account [22, 23].

218 The  $\Delta N_{\text{ch}}$  distributions are characterized by cumulants and related quantities such as  $\mu$ ,  $\sigma$ ,  $S$ , and  $\kappa$ , which are  
 219 calculated from the distributions. The statistical uncertainties for the cumulants are calculated using the bootstrap  
 220 method [24]. Corrections are then made for the reconstruction efficiency, which is estimated for each centrality and  
 221 energy using the HIJING1.37 event generator [25] and then processed through a GEANT simulation with the PHENIX  
 222 detector setup. For all collision energies, the average efficiency for detecting the particles within the acceptance varies  
 223 between 65%–72% and 76%–85% for central (0%–5%) and peripheral (55%–60%) events, respectively with 4%–5%  
 224 variation as a function of energy. The efficiency correction applied to the cumulants is based on a binomial probability  
 225 distribution for the reconstruction efficiency [26]. The efficiency corrected  $\mu$ ,  $\sigma$ ,  $S$ , and  $\kappa$  as a function of  $\langle N_{\text{part}} \rangle$   
 226 are shown in panels (c-f) of Fig. 1.

227 The  $\mu$  and  $\sigma$  for net-charge distributions increase with increasing  $\langle N_{\text{part}} \rangle$ , while  $S$  and  $\kappa$  decrease with increasing  
 228  $\langle N_{\text{part}} \rangle$  for all collision energies. At a given  $\langle N_{\text{part}} \rangle$  value,  $\mu$ ,  $S$ , and  $\kappa$  of net-charge distributions decrease with

229 increasing collision energy. However, the width ( $\sigma$ ) of net-charge distributions increases with increasing collision  
 230 energy indicating the increase of fluctuations in the system at higher  $\sqrt{s_{NN}}$ .

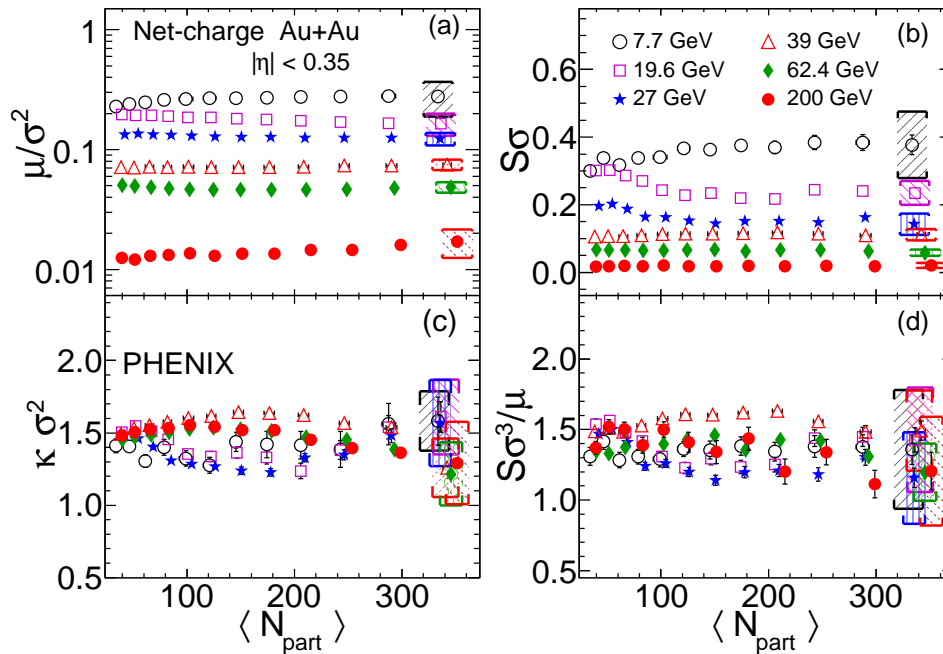


FIG. 2. (Color online).  $\langle N_{part} \rangle$  dependence of efficiency corrected (a)  $\mu/\sigma^2$ , (b)  $S\sigma$ , (c)  $\kappa\sigma^2$ , and (d)  $S\sigma^3/\mu$  of net-charge distributions for Au+Au collisions at different collision energies. Statistical errors are shown along with the data points while systematic uncertainties are shown for (0%–5%) collisions.

231 The systematic uncertainties are estimated by: (1) varying the  $Z_{vertex}$  cut to less than  $\pm 10$  cm; (2) varying the  
 232 matching parameters of PC3 hits and EMCal clusters with the projected tracks to study the effect of background  
 233 tracks originating from secondary interactions or from ghost tracks; (3) varying the centrality bin width to study  
 234 nondynamical contributions to the net-charge fluctuations due to the finite width of the centrality bins [27–29]; and  
 235 (4) varying the lower  $p_T$  cut. The total systematic uncertainties estimated for various cumulants for all energies are:  
 236 10%–24% for  $\mu$ , 5%–10% for  $\sigma$ , 25%–30% for  $S$ , and 12%–19% for  $\kappa$ . The systematic uncertainties are similar for all  
 237 centralities at a given energy and are treated as uncorrelated as a function of  $\sqrt{s_{NN}}$ . For clarity of presentation, the  
 238 systematic uncertainties are only shown for central (0%–5%) collisions.

239 Figure 2 shows the  $\langle N_{part} \rangle$  dependence of  $\mu/\sigma^2$ ,  $S\sigma$ ,  $\kappa\sigma^2$ , and  $S\sigma^3/\mu (= (S\sigma)/(\mu/\sigma^2))$  extracted from the net-charge  
 240 distributions in Au+Au collisions at different  $\sqrt{s_{NN}}$ . The results are corrected for the reconstruction efficiencies.  
 241 Statistical uncertainties are shown along with the data points. The systematic uncertainties are constant fractional  
 242 errors for all centralities at a particular energy, hence they are presented for the central (0%–5%) collision data point  
 243 only. The systematic uncertainties on these ratios across different energies varies as follows: 20%–30% for  $\mu/\sigma^2$ ,  
 244 15%–34% for  $S\sigma$ , 12%–22% for  $\kappa\sigma^2$ , and 17%–32% for  $S\sigma^3/\mu$ . It is observed in Fig. 2 that the ratios of the cumulants  
 245 are weakly dependent on  $\langle N_{part} \rangle$  for each collision energy; the values of  $\mu/\sigma^2$  and  $S\sigma$  decrease from lower to higher  
 246 collision energies, while the  $\kappa\sigma^2$  and  $S\sigma^3/\mu$  values are constant as a function of  $\sqrt{s_{NN}}$  within systematic uncertainties.

247 The collision energy dependence of  $\mu/\sigma^2$ ,  $S\sigma$ ,  $\kappa\sigma^2$  and  $S\sigma^3/\mu$  of the net-charge distributions for central (0%–  
 248 5%) Au+Au collisions are shown in Fig. 3. The statistical and systematic uncertainties are shown along with the  
 249 data points. The experimental data are compared with negative-binomial-distribution (NBD) expectations, which  
 250 are calculated by computing the efficiency corrected cumulants for the measured  $N^+$  and  $N^-$  distributions fit with  
 251 NBD's respectively, which also describe total charge ( $N^+ + N^-$ ) distributions very well [27, 28]. The various order  
 252 ( $n = 1, 2, 3$  and 4) of net-charge cumulants from NBD are given as  $C_n(\Delta N_{ch}) = C_n(N^+) + (-1)^n C_n(N^-)$ , where  
 253  $C_n(N^+)$  and  $C_n(N^-)$  are cumulants of  $N^+$  and  $N^-$  distributions, respectively [30, 31].

254 The  $\mu/\sigma^2$  and  $S\sigma$  values in Fig. 3(a) and Fig. 3(b), respectively both decrease with increasing  $\sqrt{s_{NN}}$ . The NBD  
 255 expectation agrees well with the data. The  $\kappa\sigma^2$  values in Fig. 3(c) remain constant and positive, between  $1.0 <$   
 256  $\kappa\sigma^2 < 2.0$  at all the collision energies within the statistical and systematic uncertainties. However, there is  $\sim 25\%$   
 257 increase of  $\kappa\sigma^2$  values at lower energies compared to higher energies above  $\sqrt{s_{NN}} = 39$  GeV, which is within the  
 258 systematic uncertainties. These data are in agreement with a previous measurement [32], but provide a more precise  
 259 determination of the higher cumulant ratios, verified by the NBD method of correcting for efficiency, which is simple

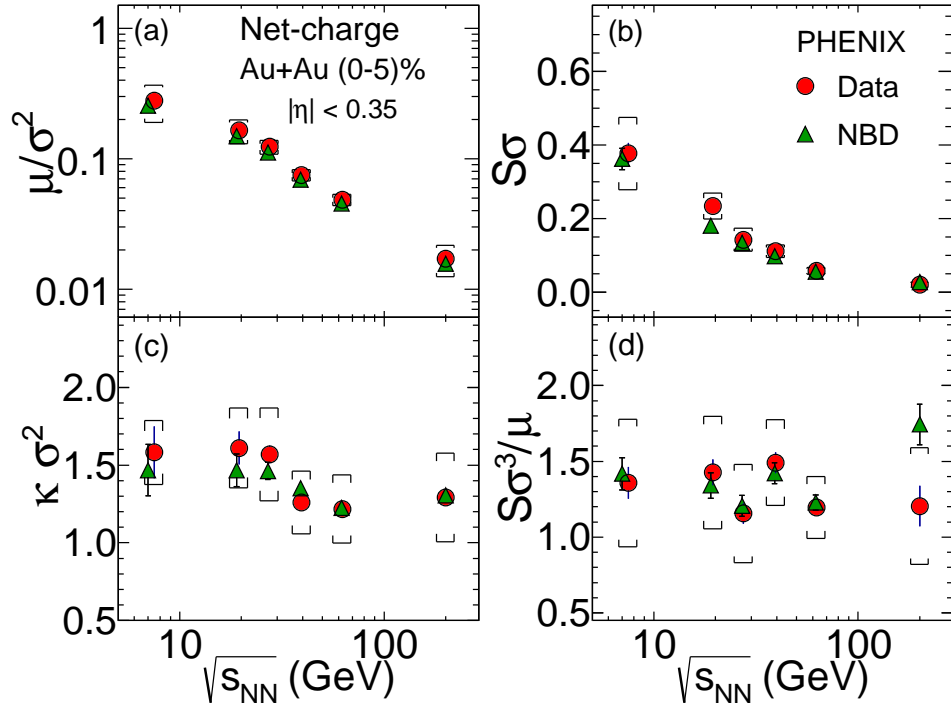


FIG. 3. (Color online). The energy dependence of efficiency corrected (a)  $\mu/\sigma^2$ , (b)  $S\sigma$ , (c)  $\kappa\sigma^2$ , and (d)  $S\sigma^3/\mu$  of net-charge distributions for central (0%–5%) Au+Au collisions. The error bars are statistical and caps are systematic uncertainties. The triangle symbol shows the corresponding efficiency corrected cumulant ratios for net-charge, from NBD fits to the individual  $N^+$  and  $N^-$  distributions.

260 and analytical for all cumulant ratios with the standard binomial correction [26]. The  $S\sigma^3/\mu$  values in Fig. 3(d)  
 261 remain constant at all collision energies within the uncertainties and are well described by the NBD expectation.  
 262 From the energy dependence of  $\mu/\sigma^2$ ,  $S\sigma$ ,  $\kappa\sigma^2$ , and  $S\sigma^3/\mu$ , no obvious nonmonotonic behavior is observed. Although  
 263 both previous measurements by STAR [32, 33] use the pseudorapidity range  $|\eta| \leq 0.5$ , compared to the present  
 264 measurement spanning  $|\eta| \leq 0.35$ , these measurements are all within the central rapidity region and are expected to  
 265 be valid for comparison to lattice QCD calculations. The efficiency corrected results for the cumulant ratios  $\mu/\sigma^2$ ,  $S\sigma$ ,  
 266 and  $\kappa\sigma^2$  remain the same within statistics whether each single arm of the PHENIX central spectrometer (azimuthal  
 267 aperture  $\delta\phi = \pi/2$ ) or both arms ( $\delta\phi = \pi$ ) are used. This is a clear verification of the insensitivity of measured  
 268 cumulant ratios to volume effects.

TABLE I. Freeze-out  $T_f$  and  $\mu_B$  vs.  $\sqrt{s_{NN}}$  in the range  $27 \leq \sqrt{s_{NN}} \leq 200$  GeV from this work compared to  $\mu_B$  values from Ref. [35], which used STAR net-charge cumulant measurements from Ref. [32] for  $\mu_B$ ; with  $140 \text{ MeV} \leq T_f \leq 150 \text{ MeV}$  obtained from STAR net-proton measurement in Ref. [33] by averaging  $S\sigma^3/\mu$  over  $\sqrt{s_{NN}} = 27, 39, 62.4$  and 200 GeV.

$\sqrt{s_{NN}}$ (GeV)	PHENIX + Ref. [14, 36]		PHENIX + Ref. [37]		STAR + Ref. [35]
	$T_f$ (MeV)	$\mu_B$ (MeV)	$T_f$ (MeV)	$\mu_B$ (MeV)	$\mu_B$ (MeV)
27	$164 \pm 6$	$181 \pm 21$	$160 \pm 6$	$184 \pm 21$	$136 \pm 13.8$
39	$158 \pm 5$	$114 \pm 13$	$156 \pm 5$	$118 \pm 10$	$101 \pm 10$
62.4	$163 \pm 5$	$71 \pm 8$	$159 \pm 5$	$74 \pm 8$	$66.6 \pm 7.9$
200	$163 \pm 8$	$27 \pm 5$	$159 \pm 8$	$25 \pm 7$	$22.8 \pm 2.6$

269 The precise measurement of both  $\mu/\sigma^2$  and  $S\sigma^3/\mu$  in the present study allow both  $\mu_B$  and  $T_f$  to be determined,  
 270 unlike a previous calculation in Ref. [35, 37], which was only able to use the  $\mu/\sigma^2$  measurement from Ref. [32]. The  
 271 comparison of  $S\sigma^3/\mu$  for different  $\sqrt{s_{NN}}$  with the lattice calculations (Fig. 3(b) in Ref. [14, 36]) enables us to extract  
 272 the chemical freeze-out temperature ( $T_f$ ). Furthermore,  $\mu_B$  can be extracted by comparing the measured  $\mu/\sigma^2$  ratios  
 273 with the lattice calculations of  $R_{12} = \mu/\sigma^2$  (Fig.3(a) in Ref. [14, 36]). The extracted  $T_f$  and  $\mu_B$  values are listed  
 274 in Table I. The  $T_f$  and  $\mu_B$  extracted using the lattice calculations in the continuum limit from Ref. [37] are also



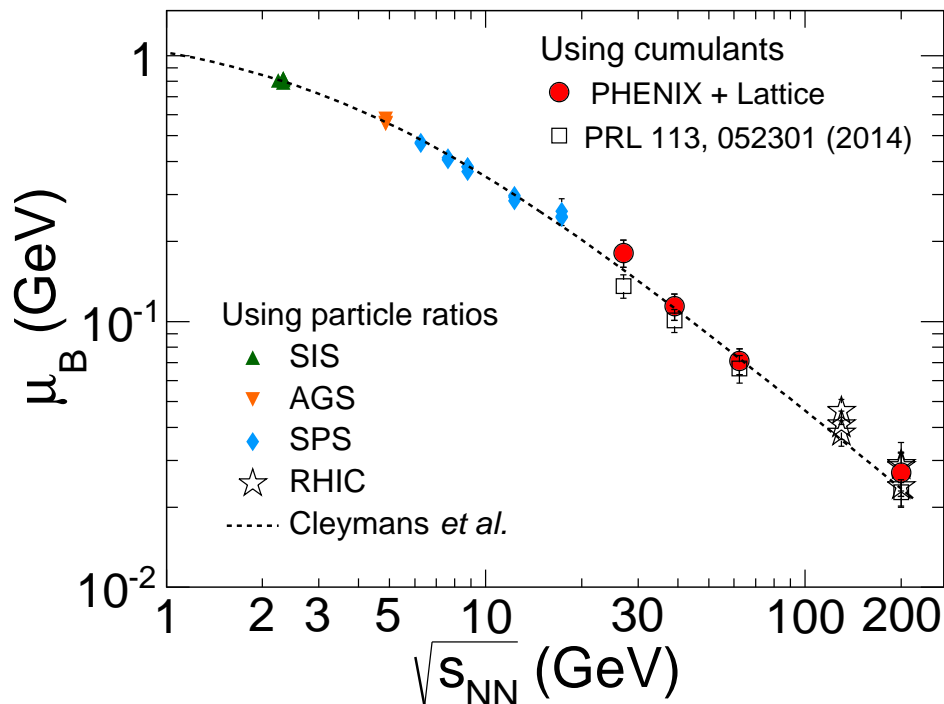


FIG. 4. (Color online). The energy dependence of the chemical freeze-out parameter  $\mu_B$ . The dashed line is the parametrization given in Ref. [34] and the other experimental data are from Ref. [34] and references therein.

depicted in Table I. The extracted freeze-out parameters using different lattice results agree very well. However, the extracted  $T_f$  are 2-4 MeV lower using Ref. [37] than with Ref. [14, 36], which is well within the stated uncertainties. The detailed freeze-out parameter extraction procedure is given in Ref. [14, 35, 37]. This is a direct combination of experimental data and lattice calculations to extract physical quantities. The  $\sqrt{s_{NN}}$  dependence of  $\mu_B$  shown in Fig. 4 is in agreement with the thermal-statistical analysis model of identified particle yields [34]. The  $\mu_B$  extracted in the present net-charge measurement and the values reported in [35] are in agreement within stated uncertainties, with some tension at  $\sqrt{s_{NN}} = 27$  GeV. Available lattice results allow extraction of  $\mu_B$  and  $T_f$  from  $\sqrt{s_{NN}} = 27$  GeV and higher using the present net-charge experimental data. Other recent calculations [38, 39] have used both net-proton and net-charge measurements to estimate the freeze-out parameters.

In summary, fluctuations of net-charge distributions have been studied using higher cumulants ( $\mu$ ,  $\sigma$ ,  $S$ , and  $\kappa$ ) for  $|\eta| < 0.35$  with the PHENIX experiment in Au+Au collisions ranging from  $\sqrt{s_{NN}} = 7.7$  to 200 GeV. The ratios of cumulants ( $\mu/\sigma^2$ ,  $S\sigma$ ,  $\kappa\sigma^2$ , and  $S\sigma^3/\mu$ ) have been derived from the individual cumulants of the distributions studied as a function of  $\langle N_{\text{part}} \rangle$  and  $\sqrt{s_{NN}}$ . The  $\mu/\sigma^2$  and  $S\sigma$  values decrease with increasing collision energy and are weakly dependent on centrality, whereas  $\kappa\sigma^2$  and  $S\sigma^3/\mu$  values remain constant over all collision energies within uncertainties. The efficiency corrected values from the NBD expectation reproduce the experimental data. These data are in agreement with a previous measurement [32], but provide more precise determination of the higher cumulant ratios  $S\sigma$  and  $\kappa\sigma^2$ . In the present study we do not observe any significant nonmonotonic behavior of  $\mu/\sigma^2$ ,  $S\sigma$ ,  $\kappa\sigma^2$ , and  $S\sigma^3/\mu$  as a function of collision energies. Comparison of the present measurements together with the lattice calculations enables us to extract the freeze-out temperature  $T_f$  and baryon chemical potential ( $\mu_B$ ) over a range of collision energies. The extracted  $\mu_B$  values are in excellent agreement with the thermal-statistical analysis model [34].

We thank the staff of the Collider-Accelerator and Physics Departments at Brookhaven National Laboratory and the staff of the other PHENIX participating institutions for their vital contributions. We thank F. Karsch and S. Mukherjee for providing us with tables of their calculations and for helpful discussions. We acknowledge support from the Office of Nuclear Physics in the Office of Science of the Department of Energy, the National Science Foundation, Abilene Christian University Research Council, Research Foundation of SUNY, and Dean of the College of Arts and Sciences, Vanderbilt University (U.S.A), Ministry of Education, Culture, Sports, Science, and Technology and the Japan Society for the Promotion of Science (Japan), Conselho Nacional de Desenvolvimento Científico e Tecnológico and Fundação de Amparo à Pesquisa do Estado de São Paulo (Brazil), Natural Science Foundation of China (People's Republic of China), Ministry of Science, Education, and Sports (Croatia), Ministry of Education, Youth and Sports (Czech Republic), Centre National de la Recherche Scientifique, Commissariat à l'Énergie Atomique, and Institut

305 National de Physique Nucléaire et de Physique des Particules (France), Bundesministerium für Bildung und Forschung,  
 306 Deutscher Akademischer Austausch Dienst, and Alexander von Humboldt Stiftung (Germany), National Science Fund,  
 307 OTKA, Károly Róbert University College, and the Ch. Simonyi Fund (Hungary), Department of Atomic Energy and  
 308 Department of Science and Technology (India), Israel Science Foundation (Israel), Basic Science Research Program  
 309 through NRF of the Ministry of Education (Korea), Physics Department, Lahore University of Management Sciences  
 310 (Pakistan), Ministry of Education and Science, Russian Academy of Sciences, Federal Agency of Atomic Energy  
 311 (Russia), VR and Wallenberg Foundation (Sweden), the U.S. Civilian Research and Development Foundation for  
 312 the Independent States of the Former Soviet Union, the Hungarian American Enterprise Scholarship Fund, and the  
 313 US-Israel Binational Science Foundation.

- 
- 314 [1] M. A. Stephanov, K. Rajagopal, and E. V. Shuryak, “Signatures of the tricritical point in QCD,” *Phys. Rev. Lett.* **81**,  
 315 4816 (1998).  
 316 [2] M. G. Alford, K. Rajagopal, and F. Wilczek, “QCD at finite baryon density: Nucleon droplets and color superconductiv-  
 317 ity,” *Phys. Lett. B* **422**, 247 (1998).  
 318 [3] M. A. Stephanov, “Random matrix model of QCD at finite density and the nature of the quenched limit,” *Phys. Rev.*  
 319 *Lett.* **76**, 4472 (1996).  
 320 [4] Y. Aoki, G. Endrodi, Z. Fodor, S.D. Katz, and K.K. Szabo, “The Order of the quantum chromodynamics transition  
 321 predicted by the standard model of particle physics,” *Nature* **443**, 675 (2006).  
 322 [5] R. D. Pisarski and F. Wilczek, “Remarks on the Chiral Phase Transition in Chromodynamics,” *Phys. Rev. D* **29**, 338  
 323 (1984).  
 324 [6] M. A. Stephanov, “QCD phase diagram and the critical point,” *Prog. Theor. Phys. Suppl.* **153**, 139 (2004).  
 325 [7] Z. Fodor and S.D. Katz, “Critical point of QCD at finite T and mu, lattice results for physical quark masses,” *J. High*  
 326 *Energy Phys.* **0404**, 050 (2004).  
 327 [8] S. Ejiri, “Canonical partition function and finite density phase transition in lattice QCD,” *Phys. Rev. D* **78**, 074507 (2008).  
 328 [9] M. A. Stephanov, K. Rajagopal, and E. V. Shuryak, “Event-by-event fluctuations in heavy ion collisions and the QCD  
 329 critical point,” *Phys. Rev. D* **60**, 114028 (1999).  
 330 [10] V. Koch, A. Majumder, and J. Randrup, “Baryon-strangeness correlations: A Diagnostic of strongly interacting matter,”  
 331 *Phys. Rev. Lett.* **95**, 182301 (2005).  
 332 [11] M. Asakawa, U. W. Heinz, and B. Muller, “Fluctuation probes of quark deconfinement,” *Phys. Rev. Lett.* **85**, 2072 (2000).  
 333 [12] M. Asakawa, S. Ejiri, and M. Kitazawa, “Third moments of conserved charges as probes of QCD phase structure,” *Phys.*  
 334 *Rev. Lett.* **103**, 262301 (2009).  
 335 [13] S. Ejiri, F. Karsch, and K. Redlich, “Hadronic fluctuations at the QCD phase transition,” *Phys. Lett. B* **633**, 275 (2006).  
 336 [14] A. Bazavov, H. T. Ding, P. Hegde, O. Kaczmarek, F. Karsch, E. Laermann, S. Mukherjee, P. Petreczky, C. Schmidt,  
 337 D. Smith, W. Soeldner, and M. Wagner, “Freeze-out Conditions in Heavy Ion Collisions from QCD Thermodynamics,”  
 338 *Phys. Rev. Lett.* **109**, 192302 (2012).  
 339 [15] M. A. Stephanov, “Non-Gaussian fluctuations near the QCD critical point,” *Phys. Rev. Lett.* **102**, 032301 (2009).  
 340 [16] R.V. Gavai and S. Gupta, “Lattice QCD predictions for shapes of event distributions along the freezeout curve in heavy-ion  
 341 collisions,” *Phys. Lett. B* **696**, 459 (2011).  
 342 [17] M. Cheng, P. Hegde, C. Jung, F. Karsch, O. Kaczmarek, E. Laermann, R. D. Mawhinney, C. Miao, P. Petreczky,  
 343 C. Schmidt, and W. Soeldner, “Baryon Number, Strangeness and Electric Charge Fluctuations in QCD at High Temper-  
 344 ature,” *Phys. Rev. D* **79**, 074505 (2009).  
 345 [18] F. Karsch and K. Redlich, “Probing freeze-out conditions in heavy ion collisions with moments of charge fluctuations,”  
 346 *Phys. Lett. B* **695**, 136 (2011).  
 347 [19] M.M. Aggarwal *et al.* (STAR Collaboration), “Higher Moments of Net-proton Multiplicity Distributions at RHIC,” *Phys.*  
 348 *Rev. Lett.* **105**, 022302 (2010).  
 349 [20] K. Adcox *et al.* (PHENIX Collaboration), “PHENIX detector overview,” *Nucl. Instrum. Methods Phys. Res., Sec. A* **499**,  
 350 469 (2003).  
 351 [21] E. Richardson *et al.* (PHENIX Collaboration), “A Reaction Plane Detector for PHENIX at RHIC,” *Nucl. Instrum. Methods*  
 352 *Phys. Res., Sec. A* **636**, 99 (2011).  
 353 [22] S.S. Adler *et al.* (PHENIX Collaboration), “Systematic studies of the centrality and  $\sqrt{s_{NN}}$  dependence of the  $d E(T) / d$   
 354  $\eta$  and  $d(N(ch) / d\eta$  in heavy ion collisions at mid-rapidity,” *Phys. Rev. C* **71**, 034908 (2005).  
 355 [23] M. L. Miller, K. Reygers, S. J. Sanders, and P. Steinberg, “Glauber modeling in high energy nuclear collisions,” *Ann.*  
 356 *Rev. Nucl. Part. Sci.* **57**, 205 (2007).  
 357 [24] B. Efron and R. J. Tibshirani, *An Introduction to the Bootstrap* (Chapman and Hall, CRC, Mortimer House, 37-41 Mortimer  
 358 Street, London, W1T 3JH., 1994) Monographs on Statistics and Applied Probability 57.  
 359 [25] X.-N. Wang and M. Gyulassy, “HIJING: A Monte Carlo model for multiple jet production in  $pp$ ,  $pA$  and  $AA$  collisions,”  
 360 *Phys. Rev. D* **44**, 3501 (1991).  
 361 [26] A. Bzdak, V. Koch, and V. Skokov, “Baryon number conservation and the cumulants of the net proton distribution,”  
 362 *Phys. Rev. C* **87**, 014901 (2013).  
 363 [27] A. Adare *et al.* (PHENIX Collaboration), “Charged hadron multiplicity fluctuations in Au+Au and Cu+Cu collisions from

- 364  $\sqrt{s_{NN}}=22.5$  to 200 GeV,” Phys. Rev. C **78**, 044902 (2008).
- 365 [28] S.S. Adler *et al.* (PHENIX Collaboration), “Measurement of density correlations in pseudorapidity via charged particle  
366 multiplicity fluctuations in Au+Au collisions at  $\sqrt{s_{NN}} = 200$  GeV,” Phys. Rev. C **76**, 034903 (2007).
- 367 [29] V.P. Konchakovski, M. I. Gorenstein, E.L. Bratkovskaya, and H. Stoecker, “Baryon number and electric charge fluctuations  
368 in pb+pb collisions at SPS energies,” Phys. Rev. C **74**, 064911 (2006).
- 369 [30] O. E. Barndorff-Nielsen, D. G. Pollard, and N. Shephard, “Integer-valued Levy processes and low latency financial  
370 econometrics,” Quantitative Finance **12**, 587 (2012).
- 371 [31] T. J. Tarnowsky and G. D. Westfall, “First Study of the Negative Binomial Distribution Applied to Higher Moments of  
372 Net-charge and Net-proton Multiplicity Distributions,” Phys. Lett. B **724**, 51 (2013).
- 373 [32] L. Adamczyk *et al.* (STAR Collaboration), “Beam energy dependence of moments of the net-charge multiplicity distribu-  
374 tions in Au+Au collisions at RHIC,” Phys. Rev. Lett. **113**, 092301 (2014).
- 375 [33] L. Adamczyk *et al.* (STAR Collaboration), “Energy Dependence of Moments of Net-proton Multiplicity Distributions at  
376 RHIC,” Phys. Rev. Lett. **112**, 032302 (2014).
- 377 [34] J. Cleymans, H. Oeschler, K. Redlich, and S. Wheaton, “Comparison of chemical freeze-out criteria in heavy-ion collisions,”  
378 Phys. Rev. C **73**, 034905 (2006).
- 379 [35] S. Borsanyi, Z. Fodor, S. D. Katz, S. Krieg, C. Ratti, and K. K. Szabo, “Freeze-out parameters from electric charge and  
380 baryon number fluctuations: is there consistency?” Phys. Rev. Lett. **113**, 052301 (2014).
- 381 [36] S. Mukherjee, “Freeze-out Condition from Lattice QCD and the Role of Additional Strange Hadrons,” (2014) p. 005,  
382 Proceedings of CPOD 2014.
- 383 [37] S. Borsanyi, Z. Fodor, S. D. Katz, S. Krieg, C. Ratti, and K. K. Szabo, “Freeze-out parameters: lattice meets experiment,”  
384 Phys. Rev. Lett. **111**, 062005 (2013).
- 385 [38] P. Alba, W. Alberico, R. Bellwied, M. Bluhm, Mantovani S. V., M. Nahrgang, and C. Ratti, “Freeze-out conditions from  
386 net-proton and net-charge fluctuations at RHIC,” Phys. Lett. B **738**, 305 (2014).
- 387 [39] A. Bazavov *et al.*, “The curvature of the freeze-out line in heavy ion collisions,” arXiv:1509.05786.